

Trimeric As^{3+}O_6 clusters in walentaite: crystal structure and revised formula

IAN EDWARD GREY^{1,*}, WILLIAM GUS MUMME¹, and RUPERT HOCHLEITNER²

¹CSIRO Mineral Resources, Private Bag 10, Clayton 3169, Victoria, Australia

²Mineralogical State Collection (SNSB), Theresienstrasse 41, 80333 München, Germany

*Corresponding author, e-mail: ian.grey@csiro.au

Abstract: The crystal structure of walentaite, originally reported as a calcium iron arsenate phosphate, has been determined and the As has been found to be predominantly in the trivalent state, as AsO_3 trigonal pyramids and as As_3O_6 trimeric clusters. The mineral has body-centred orthorhombic symmetry with $a = 26.188(5)$, $b = 7.360(2)$, $c = 10.367(2)$ Å. The structure was solved in space group *Imma* using synchrotron single-crystal diffraction data and refined to $R1 = 0.054$ for 1454 observed reflections. The walentaite structure is based on the stacking of heteropolyhedral layers along [100] with the layers held together by hydrogen bonds to interlayer hydrated cations $M(\text{H}_2\text{O})_6$, $M = \text{Mn}^{2+}$, Fe^{2+} , Ca^{2+} , Na^+ . The layers, of composition $\text{Fe}_3^{3+}(\text{P}_{0.84}\text{As}_{0.16}\text{O}_4)_2(\text{O}, \text{OH})_6$, have the same topology of corner-connected octahedra and tetrahedra as in the alunite-supergroup mineral kintoreite-1c. Unit-cell-scale twinning of the kintoreite-like layers gives a saw-tooth aspect to the layers. The AsO_3 , As_3O_6 and $(\text{Ca}, \text{Na})\text{O}_6$ groups are attached to the surface of the layers. Although the kintoreite-like heteropolyhedral layers are fully ordered in *Imma*, the surface-attached groups and the interlayer hydrated cations are highly disordered, so the *Imma* model represents the average structure. Models for the local ordering have been developed from interpretation of the partial site occupancies and splitting of the disordered atoms. The crystal structure results have been combined with electron microprobe analyses to obtain a new formula for walentaite, $\text{Fe}_3^{3+}(\text{P}_{0.84}\text{As}_{0.16}\text{O}_4)_2(\text{O}, \text{OH})_6\text{As}_{2.56}^{3+}\text{Ca}_{0.42}\text{Na}_{0.28}\text{Mn}_{0.35}^{2+}\text{Fe}_{0.30}^{2+}\text{O}_{6.1}(\text{OH})_{0.9}(\text{H}_2\text{O})_{5.2}$, in which 89% of the As is present as As^{3+} .

Key-words: walentaite; ferric arsenite phosphate; crystal structure; single crystal determination; new formula; trimeric As_3O_6 clusters; kintoreite-1c.

1. Introduction

Walentaite was described as a new calcium iron arsenate phosphate mineral from the White Elephant Mine, Pringle, South Dakota, by Dunn *et al.* (1984). From Weissenberg and precession photos they established the symmetry as body-centred orthorhombic, with possible space groups *Imam*, *Ima2*, *Imm2*, *Immm*, *I222* or *I2_12_12_1*. Refinement of the powder X-ray diffraction (XRD) data gave the parameters $a = 26.24(6)$, $b = 10.31(1)$ and $c = 7.38(1)$ Å. Dunn *et al.* noted the exceptionally small size of the bladed crystals, with thicknesses of only 1–2 µm, giving very weak XRD patterns and they were not able to proceed with a structure determination. They determined the water content directly by thermal analysis and the Fe valence state qualitatively using a micro-chemical test that indicated both Fe^{2+} and Fe^{3+} with Fe^{3+} predominant. These were combined with electron microprobe (EMP) analyses to give a unit-cell composition of ideally $\text{H}_4(\text{Ca}, \text{Mn}, \text{Fe}^{2+})_4\text{Fe}^{3+}_{12}(\text{AsO}_4)_{10}(\text{PO}_4)_6 \cdot 28\text{H}_2\text{O}$. The authors noted that the “formula must be considered tentative pending structural study”.

Using synchrotron XRD data collected on a single crystal, we have determined the structure for walentaite and have found that the As is present predominantly (89%) as As^{3+} ,

requiring a revision of the Dunn *et al.* (1984) formula. We report here the results of the crystal structure analysis and the resulting revised formula.

2. Experimental procedure

2.2. Sample and analyses

We were not successful in being able to obtain a sample of the type material. Instead, the sample used for the study was from the White Elephant Mine type locality, provided by Christian Rewitzer. The walentaite occurs as small radial aggregates of bright yellow blades on quartz. The crystals used for the data collection and electron microprobe analyses were obtained by lightly crushing one of the aggregates to liberate the individual blades. The crystals were inspected optically. Under polarized light the crystals showed very fine-scale (sub-micrometre) colour zoning, affecting the sharpness of the extinction.

Crystals of walentaite (7 crystals) were analysed using wavelength-dispersive spectrometry on a JEOL JXA 8500F Hyperprobe operated at an accelerating voltage of 15 kV and a beam current of 2.5 nA. The beam was defocused to 4 µm. Standards were scorodite (Fe and As),

Table. 1 Data collection and refinement conditions for walentaite.

Formula	$\text{As}_{2.88}\text{H}_{11.30}\text{Ca}_{0.42}\text{Fe}_{3.30}\text{Mn}_{0.35}\text{Na}_{0.28}\text{O}_{20.20}\text{P}_{1.68}$
Formula mass	829.2
Temperature	100 K
Wavelength	0.7107 Å
Crystal system, space group	Orthorhombic, <i>Imma</i>
Unit-cell dimensions	$a = 26.188(5)$ Å $b = 7.3600(15)$ Å $c = 10.367(2)$ Å 1998.2(7) Å ³ 4, 2.756 g cm ⁻³ 7.642 mm ⁻¹ 0.01 × 0.02 × 0.002 mm
Volume	0.7 Å
Z, Calculated density	17,665/1612 [$R(\text{int}) = 0.071$]/1454
Absorption coefficient	100.00%
Crystal size	Full-matrix least-squares on F^2
Data resolution	1612/0/127
Reflections collected/unique/observed	1.154
Completeness to $\theta = 25.242$	$R_1 = 0.0537$, $wR_2 = 0.1699$
Refinement method	$R_1 = 0.0578$, $wR_2 = 0.1732$
Data/restraints/parameters	0.0007(2)
Goodness-of-fit on F^2	1.53 and -0.97 e.Å ⁻³
Final R indices [$I > 2\sigma(I)$]	
R indices (all data)	
Extinction coefficient	
Largest diff. peak and hole	

wollastonite (Ca), albite (Na), synthetic MnSiO₃ (Mn) and AlPO₄ (P). Results: Fe₂O₃ 28.1, As₂O₅ 38.1, P₂O₅ 12.9, MnO 2.69, CaO 2.55, Na₂O 0.90, total 85.2 wt%. For comparison, Dunn *et al.* (1984) obtained Fe₂O₃ 28.3, FeO 3.2, As₂O₅ 32.9, P₂O₅ 12.5, MnO 3.1, CaO 2.9, Al₂O₃ 0.5, after scaling their analyses to 100% with the inclusion of 16.6 wt% H₂O. Dunn *et al.* did not report a Na analysis.

2.3. X-ray data collection and structure analysis

A synchrotron single-crystal data collection was obtained on the macromolecular beam line MX2 of the Australian Synchrotron. Data were collected at 100 K using an ADSC Quantum 315r detector and monochromatic radiation with a wavelength of 0.7107 Å. The data set was integrated using a primitive triclinic cell and a search for higher symmetry gave an *I*-centred orthorhombic cell with parameters very close to those reported by Dunn *et al.* (1984), with *b* and *c* interchanged to correspond to the centrosymmetric space-group setting *Imma*, giving *a* = 26.188(5), *b* = 7.360(2), *c* = 10.367(2) Å.

Structure solutions in *Imma* and the non-centrosymmetric space groups *Ima2*, *Imm2* and *I2*₁*2*₁*2*₁ were obtained using SHELXT (Sheldrick, 2015), implemented in WinGX (Farrugia, 1999). All models had high values of *R*1 (>20%) and all showed the same features, comprising heteropolyhedral slabs of corner-connected Fe³⁺-centred octahedra and PO₄ tetrahedra parallel to (100) with disordered distributions of cations between the layers. The normalised intensity statistics indicated centrosymmetry ($[E^2 - 1] = 0.904$), compared with ideal values of 0.968 for centric and 0.736 for acentric) so the *Imma* model was pursued. Two independent sites for As atoms were identified adjacent to the surface of the heteropolyhedral slabs, both with pyramidal coordination indicative of As³⁺. Additionally, the observation of elongated P–O bond lengths and a

site occupancy factor greater than 1 for the P site suggested partial substitution of As⁵⁺ for P. Difference-Fourier maps were used to locate partially occupied interlayer atoms. From bond-length and coordination considerations, the disordered interlayer cation sites were resolved into separate adjacent sites for Fe/Mn (with octahedral coordination) and Ca (with edge-shared square antiprismatic coordination). A further partially occupied site for Ca was located on the surface of the heteropolyhedral slabs.

Refinement of the structure in space group *Imma* was made using SHELXL (Sheldrick, 2015). Refinement with anisotropic displacement parameters for all atoms except some oxygen (H₂O) and Ca sites with low partial occupancies converged at *R*1 = 0.054 for 1454 observed reflections with *I* > 2σ(*I*). Further details of the data collection and refinement are given in Table 1. Refined coordinates and equivalent isotropic displacement parameters are reported in Table 2, anisotropic displacement parameters in Table 3 and polyhedral bond distances in Table 4. Also included in Table 4 are the short separations between disordered atoms.

In the *Imma* model, only the FeO₆ and PO₄ of the heteropolyhedral layers are ordered and fully occupied. The disordered sites are of two types: the two independent As³⁺ sites, As2 and As3, are displaced from special positions, whereas the interlayer cations and their associated anions occupy different independent sites, separated by ~1.3 Å, with partial occupancy so only one of the sites can be occupied locally. The As2 site is split into pairs of atoms displaced by 0.23 Å from the special position 8(f) on the two-fold axis at (x 0 0), while the As3 site is split into four atoms, each displaced by 0.88 Å from the special position 4(d) (1/4 1/4 1/4). Lowering the space-group symmetry to *Imm2* allows the split As2 and As3 sites to be separated into two independent sites, but each of the two As3 sites remain split into pairs. The highest symmetry that allows separation of the As3 sites into four independent sites is monoclinic

Table 2. Refined coordinates ($\times 10^4$), equivalent isotropic displacement parameters ($\times 10^3$) and site occupation factors (*sof*) for walentaite.

Atom	Site	<i>sof</i>	<i>x</i>	<i>y</i>	<i>z</i>	<i>U</i> _{eq} (Å ²)
Fe1	4(c)	0.25	2500	2500	2500	24(1)
Fe2	8(f)	0.50	3244(1)	5000	5000	24(1)
P1	8(i)	0.421(3)	3742(1)	2500	2809(1)	28(1)
As1	8(i)	0.079(3)	3742(1)	2500	2809(1)	28(1)
As2	16(j)	0.396(3)	2121(1)	274(2)	5106(3)	30(1)
As3	16(j)	0.240(3)	2698(1)	3025(2)	6925(2)	26(1)
Mn1	4(e)	0.163(3)	5000	7500	2947(4)	59(1)
Ca1	4(e)	0.064(3)	5000	7500	1681(8)	33(3)
Ca2	8(f)	0.113(5)	1851(5)	0	5000	45(3)
O1	8(i)	0.50	4206(2)	2500	1912(5)	43(1)
O2	8(i)	0.50	3237(2)	2500	1993(5)	42(1)
O3	16(j)	1.00	3748(1)	4238(4)	3703(3)	33(1)
O4A	16(j)	0.36(5)	2656(11)	5380(30)	6280(30)	25(2)
O4B	16(j)	0.64(5)	2595(7)	5710(30)	6080(18)	25(2)
O5	8(i)	0.50	3207(2)	2500	5771(4)	28(1)
O6	8(i)	0.26(1)	2111(3)	2500	5938(10)	35(3)
OW1A	8(i)	0.22(1)	5716(5)	7500	3193(14)	40(4)
OW1B	8(i)	0.20(1)	5858(6)	7500	2577(17)	45(5)
OW2A	8(h)	0.28(1)	5000	4560(16)	2751(10)	49(3)
OW2B	8(h)	0.167(7)	5000	5160(30)	1880(20)	72(7)
OW3	16(j)	0.09(1)	5220(20)	7500	4830(50)	99(21)
OW4	4(e)	0.08(1)	0	2500	5870(40)	62(12)
OW5	16(j)	0.25(2)	4387(9)	5500(40)	280(30)	84(9)

Table 3. Anisotropic displacement parameters ($\times 10^3$) for walentaite.

Atom	<i>U</i> ¹¹	<i>U</i> ²²	<i>U</i> ³³	<i>U</i> ²³	<i>U</i> ¹³	<i>U</i> ¹²
Fe1	33(1)	21(1)	18(1)	0	-1(1)	0
Fe2	32(1)	18(1)	24(1)	0(1)	0	0
P1	30(1)	26(1)	27(1)	0	4(1)	0
As2	34(1)	29(1)	27(1)	-1(1)	1(1)	3(1)
As3	35(1)	19(1)	25(1)	2(1)	4(1)	2(1)
Mn1	76(2)	35(2)	68(2)	0	0	0
O1	42(3)	49(3)	38(2)	0	8(2)	0
O2	33(2)	62(3)	31(2)	0	4(2)	0
O3	37(2)	23(1)	39(2)	2(1)	8(1)	-1(1)
O4A	29(4)	22(5)	24(5)	-3(4)	-1(3)	3(3)
O4B	29(4)	22(5)	24(5)	-3(4)	-1(3)	3(3)
O5	39(2)	19(2)	26(2)	0	1(2)	0
O6	35(5)	22(4)	50(6)	0	12(4)	0

Im11 (*Cm*). Structural models were obtained using SHELXT in both *Imm2* and *Cm* space groups (with merohedral twinning) in an attempt to have fully ordered (unsplitted) As2 and As3 polyhedra. It was found, however, that the other As2 and the other three As3 sites were populated with the same electron density, mimicking the split sites of the *Imma* model. This suggests that the crystals are most likely composed of small domains with different site distributions, so only the average structure over the different domains can be obtained from the refinement.

3. Results and discussion

3.1. Description of the structure

Walentaite has a structure based on the stacking of heteropolyhedral layers along [100] with a separation = 0.5a

Table 4. Polyhedral distances and short separations between disordered atoms (Å).

Fe1–O2 ×2	2.000(5)	Fe2–O3 ×2	1.965(3) ×2
–O4A ×4*	2.05(3)	–O4A ×2*	2.05(3) ×2
–O4B ×4*	1.99(1)	–O4B ×2	2.10(1) ×2
		–O5 ×2	2.008(2) ×2
P1–O1	1.531(5)	As2–O4B	1.75(2)
–O2	1.570(5)	–O4B	1.78(2)
–O3 ×2	1.580(3)	–O6	1.852(5)
Mn1–Ow1A ×2*	1.89(1)	As3–O4A	1.86(3)
–Ow1B ×2*	2.28(2)	–O5	1.833(5)
–Ow2A ×2*	2.17(1)	–O6	1.89(1)
–Ow2B ×2*	2.04(2)		
–Ow3	2.04(6)		
–Ow4	2.16(4)		
Ca1–Ow1A ×2*	2.44(1)	Ca2–O2 ×2	2.776(4)
–Ow1B ×2*	2.43(1)	–O4A ×2*	2.51(3)
–Ow2A ×2	2.43(1)	–O4B ×2*	2.31(2)
–Ow5 ×2	2.62(3)	–O6 ×2	2.189(7)
As2–As2	0.458(3)	O4A–O4B	0.36(1)
As3–As3	0.773(3)	Ow1A–Ow1B	0.74(2)
As3–As3	1.580(3)	Ow2A–Ow2B	1.01(2)
As3–As3	1.758(3)	Ow3–Ow3	1.2(2)
Ca1–Mn1	1.319(9)	Ow5–Ow5	0.93(5)
Ca2–As2	0.74(1)		

*Disordered atoms *nA* and *nB* cannot be both present in same polyhedron.

of 13.09 Å. Hydrated cation polyhedra are located between the layers and are H-bonded to the layers. The layers are illustrated in Fig. 1. The corner-connected FeO₆ octahedra form hexagonal rings (Fig. 1a) and have the same topology as a

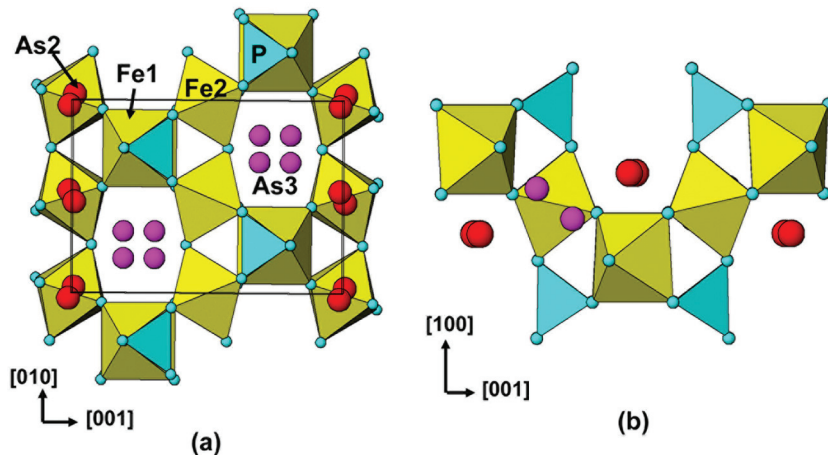


Fig. 1. Heteropolyhedral layers in walentaite; (a) [100] projection, (b) [010] projection. The disordered As2 and As3 atoms in *Imma* are shown.

(110) slice of the pyrochlore structure. The PO_4 tetrahedra each share three basal anions with three FeO_6 octahedra, giving the same topology as in the alunite super-group mineral kintoreite-1c, $\text{PbFe}_3(\text{PO}_4)_2(\text{OH},\text{H}_2\text{O})_6$ (Kharisun *et al.*, 1997; Bayliss *et al.*, 2010). The heteropolyhedral assemblage, with composition $\text{Fe}_3(\text{PO}_4)_2\Phi_6$, $\Phi = \text{O}^{2-}/\text{OH}^-$, can be described as unit-cell twinned kintoreite, with the twin plane $\{001\}$, giving a characteristic saw-tooth layer shown in Fig. 1b. The crystal-structure refinement gave 16% replacement of P by As in the tetrahedra.

The locations of the two As^{3+} cations relative to the $\text{Fe}_3(\text{PO}_4)_2\Phi_6$ layer are given in Fig. 1a, showing the splitting of As2 into pairs and As3 into quadruplets. In Fig. 2, only one of each of the split As2 and As3 atoms is plotted, corresponding to a local ordering that can be described in space group *Cm*, with the As–O bonds shown. The As_2O_3 trigonal pyramids form corner-linked dimers that share edges with successive octahedra in corner-connected octahedral chains along [010]. The average As2–O distance, 1.79 Å and O–As2–O angle, 94.9°, lie within the ranges reported by Hawthorne (1985) for 11 arsenite minerals, for which $\langle \text{As}–\text{O} \rangle = 1.78(1)$ and $\langle \text{O}–\text{As}–\text{O} \rangle = 97(2)^\circ$. The As_3O_3 trigonal pyramid shares an edge with an As_2O_3 pyramid of the dimer, forming trimeric clusters of composition $\text{As}_2\text{As}_3\text{O}_6$. This unusual geometry involves all three As^{3+} cations sharing a common anion, O6. The severe valency oversaturation at O6 is accommodated by lengthening of the As2–O6 and As3–O6 distances, see Table 4. In fact, all three As3–O distances are considerably longer than are reported for arsenite minerals. It is worth noting however that the oxygen atoms bonded to As3 have some large anisotropic displacement parameters in the range 0.03–0.05 Å² (Table 3) that correspond to local root-mean-square atomic displacements up to 0.2 Å in response to the locations of the different split As3 positions, whereas the bond distances in Table 4 correspond only to the centroids of the various displacements.

The interlayer polyhedra are of two types, depending on whether they are centred by Mn/Fe (Fig. 3) or by Ca/Na (Fig. 4). In both cases, the polyhedral anions bond only to

the central cation and so can confidently be assigned as H_2O . The Mn/Fe-centred hydrated species have octahedral coordination, although the anions Ow3 and Ow4 have less than full occupancy relative to the central cation (Mn1 in Table 2), so that some 5-coordination probably occurs. The Mn1–Ow bond distances (Table 4) are consistent with a mix of Mn^{2+} and Fe^{2+} in the polyhedra. The Ca1-centred polyhedra are square antiprisms, which share edges to form crankshaft-like chains along [010], with composition $(\text{Ca},\text{Na})(\text{H}_2\text{O})_4(\text{H}_2\text{O})_{4/2} \equiv [(\text{Ca},\text{Na})(\text{H}_2\text{O})_6]^{n+}$. Edge-sharing of Ca/Na-centred square antiprisms has been reported from a neutron diffraction study of the zeolite thomsonite (Pluth *et al.*, 1985). The anions forming the shared edges, Ow5 in Tables 2 and 4, are displaced by 0.46 Å from the special position 8(f) ($x, \frac{1}{2}, 0$). The undisplaced Ow5 would have long bond distances of 2.99 Å to Ca/Na, whereas the displacement results in shorter distances of 2.62(2) Å, comparable with the distances in thomsonite.

The site occupancy factors in Table 2 indicate that the As2 sites are only ~80% occupied (0.396(3)/0.5), whereas the As3 sites in the hexagonal rings are almost fully occupied (0.240(3)/0.25). A difference-Fourier map gave a strong peak located only 0.74(1) Å from As2, so it can only be occupied when the As2 site is vacant. Assigning Ca to the site (Ca2 in Table 2) resulted in a refined site occupancy for Ca2 of 0.113(5), consistent with Ca2 being present when the As2 site is vacant. The Ca2 atoms have one-sided coordination as shown in Fig. 4, with six Ca2–O distances in the range 2.19–2.78 Å. A seventh distance, to Ow5, is much longer at 3.27 Å. One-sided coordination to Ca and Na occurs in zeolites (Mortier, 1977; Wang & Jacobson, 1999).

3.2. Compositional considerations

The site-occupancy results are consistent with there being two types of compositional domains in the walentaite crystals. The dominant domains, representing 80% of the crystals, correspond to the regions where the As2 sites are occupied and the heteropolyhedral layers have $\text{As}_2\text{As}_3\text{O}_6$

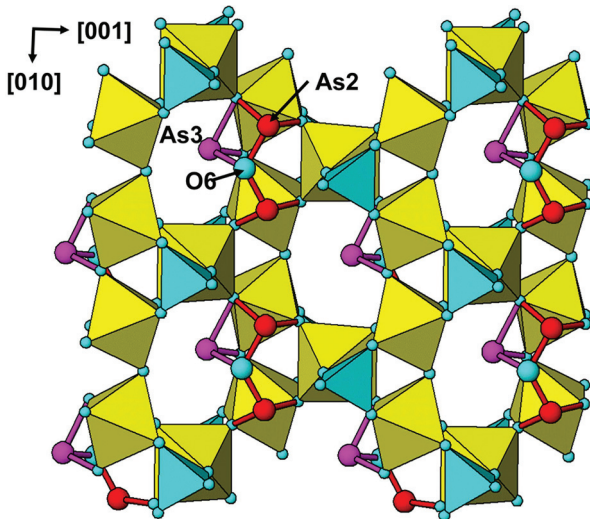
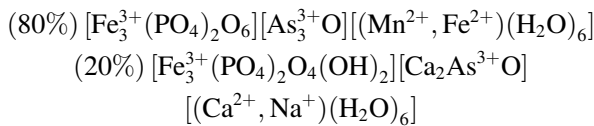


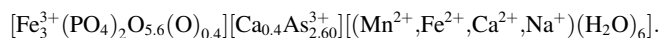
Fig. 2. [100] view of the heteropolyhedral layer in walentaite, with a locally-ordered arrangement of As_3O_6 trimeric clusters attached to the layer.

trimeric clusters attached. Site occupancy considerations indicate that the interlayer region is populated with $[(\text{Mn}^{2+}, \text{Fe}^{2+})(\text{H}_2\text{O})_6]^{2+}$ hydrated cations as shown in Fig. 3. The Mn1 site occupancy factor (0.163(3)) corresponds to occupancy of only 81% occupancy of the interlayer sites in the dominant domains; the remaining 19% of interlayer sites in the dominant domains are either empty or populated with $[(\text{Ca}, \text{Na})(\text{H}_2\text{O})_6]^{n+}$ hydrated cations. The domains corresponding to the remaining 20% of the crystals have isolated As_3O_3 trigonal pyramids attached to the heteropolyhedral layers and one-sided Ca^{2+} -centred polyhedra in place of the As_2O_6 dimers. The interlayer region in these domains is populated with $[(\text{Ca}, \text{Na})(\text{H}_2\text{O})_6]^{n+}$ hydrated cations as shown in Fig. 4. In both domains the heteropolyhedral layers are held together by H-bonding from the coordinated interlayer H_2O molecules to polyhedral anions on the surface of the layers. The H-bonds involve O1 (apical oxygen of PO_4) and O3 (shared between O1 and Fe2) as acceptors and Ow1/Ow1A and Ow2/Ow2A as donors, with O...O distances in the range 2.71–2.86 Å.

From the structure analysis, the ideal (full cation-site occupancies) compositions of the two domains are:



where the first square brackets enclose the heteropolyhedral layer composition, the second enclose the surface groupings involving As^{3+} and Ca (with possible Na), and the third enclose the interlayer hydrated cations. The overall formula is:



Taking into account the structure refinement results showing partial substitution of the P site by As^{5+} , incomplete occupancy of the interlayer hydrated cation sites by Mn^{2+}

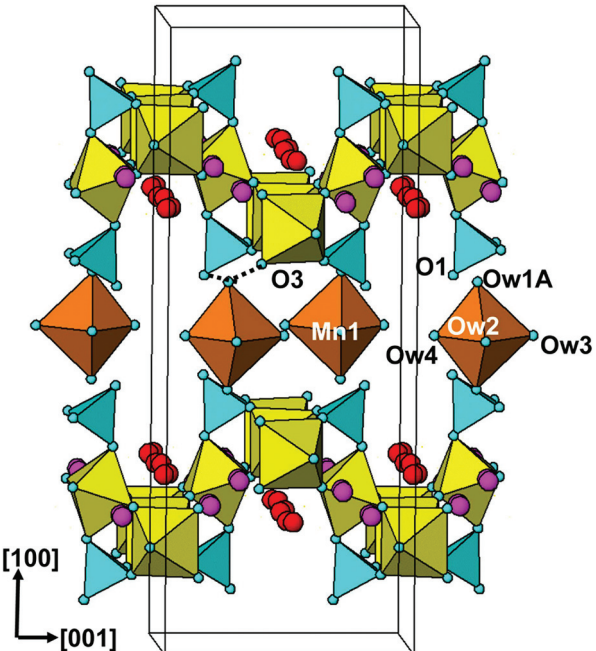
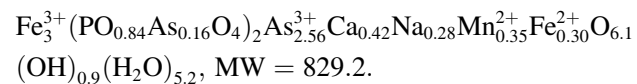
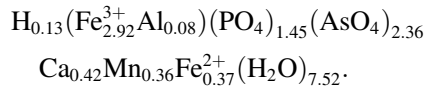


Fig. 3. Slightly offset [010] projection of the walentaite structure showing the interlayer hydrated cations centred by Mn1 (= Mn/Fe) in the dominant (80%) compositional domains. Dotted lines show H-bonds.

and Fe^{2+} , and a total of 20.2 anions ($\text{O}^{2-} + \text{OH}^- + \text{H}_2\text{O}$) *pftu*, as well as the EMP results for minor elements Mn, Na and Ca, the formula for walentaite is:



The calculated density based on this formula is 2.76 g cm⁻³, which agrees well with the Dunn *et al.* (1984) experimental density of 2.72 g cm⁻³. The new formula can be compared with the empirical formula given by Dunn *et al.* (1984), scaled to 3($\text{Fe}^{3+} + \text{Al}$) of:



The greatest discrepancy between the two formulae is due to Dunn *et al.* assuming that all As is present as As^{5+} , whereas the crystal-structure analysis shows that only 11% of the As is pentavalent, substituting for P, while 89% of the As is present as As^{3+} with pyramidal coordination.

Nickel (1987) has reported a tungsten-bearing walentaite from the Griffins Find gold deposit in Western Australia. It has the same powder pattern as walentaite and a similar orthorhombic unit cell. Nickel gave a chemical formula, based on EMP analyses, with all Fe assumed to be Fe^{3+} and with the H_2O calculated from the shortfall in the EMP oxide analyses. Scaling Nickel's formula to 2 P gives: $\text{Fe}_{2.73}^{3+}\text{W}_{0.54}(\text{PO}_4)_2(\text{AsO}_4)_{1.87}\text{Ca}_{0.35}(\text{OH})_{0.52}(\text{H}_2\text{O})_{7.68}$. The mineral has W^{6+} substituting for Fe^{3+} , and has a considerably lower As-to-P ratio than in walentaite.

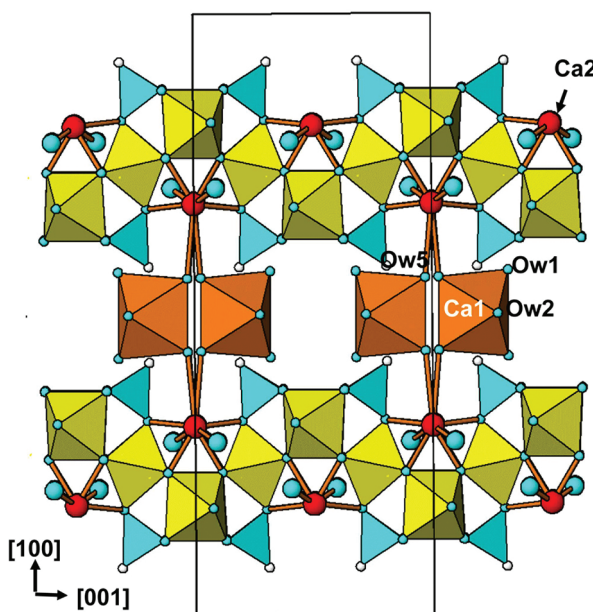


Fig. 4. [010] projection of the walentaite structure showing the interlayer hydrated cation polyhedra centred by Ca1 (= Ca/Na) and surface-coordinated Ca2 in the minor (20%) compositional domains.

We have collected synchrotron diffraction data on a crystal from the Griffins Find sample and find that, as for walentaite, the As is present predominantly as As^{3+} rather than As^{5+} . The diffraction quality of the crystals is quite poor and they suffer from the same disorder as occurs in walentaite with different compositional regions. We also find that the Griffins Find sample has dominant Na replacing Ca (Na was not analysed for by Nickel) and so is potentially a new mineral.

4. Conclusions

Walentaite presents particular challenges in determining the crystal structure because of compositional and atom positional disorder that could not be adequately modelled by symmetry lowering. As a consequence, the model presented here, in space group *Imma*, represents the average structure. The *Imma* model completely describes the ordering of saw-tooth layers of corner-connected FeO_6 and $(\text{P},\text{As})\text{O}_4$ tetrahedra that are the main building blocks of the structure. The *Imma* model, however, gives disordering of As^{3+}O_3 trigonal pyramids and CaO_6 polyhedra on the surface of the layers and disordering of $(\text{Mn}^{2+},\text{Fe}^{2+})(\text{H}_2\text{O})_6$ and $(\text{Ca}^{2+},\text{Na}^+)(\text{H}_2\text{O})_6$ hydrated cations in the interlayer regions. Lowering the symmetry to *Imm2* allows positional ordering of one of the As^{3+} cations ($\text{As}2$) but the second independent As^{3+} cation, $\text{As}3$, remains split over two positions separated by 0.77 Å. The $\text{As}3$ positions can be separated into independent sites by lowering the symmetry to *Cm*. Refinement in the lower-symmetry space groups, however, produced “ghost” atoms at the positions occupied by the split atoms in *Imma*. One of the consequences of the positional disorder of $\text{As}3$ and its coordinated oxygen atoms is that the refinement

gives only the weighted centroids of the displaced atoms and results in $\text{As}3-\text{O}$ bond distances that are longer by up to 0.1 Å than usually reported for arsenite minerals.

Regardless of the space-group symmetry used in the refinement, the additional problem of compositional disorder remains, in which 80% of the crystal volume has As_3O_6 trimeric clusters attached to the layer surfaces and $(\text{Mn}^{2+},\text{Fe}^{2+})(\text{H}_2\text{O})_6$ hydrated interlayer cations, while 20% of the volume has isolated AsO_3 pyramids and $(\text{Ca},\text{Na})\text{O}_6$ polyhedra attached to the layer surfaces and $(\text{Ca}^{2+},\text{Na}^+)(\text{H}_2\text{O})_6$ hydrated cations in the interlayer regions. Preliminary structural studies on a tungsten-bearing walentaite from Western Australia indicate that the same problems of compositional and atom positional disorder are present as in the walentaite from South Dakota.

Acknowledgements: Thanks to Christian Rewitzer for providing a sample of the type specimen of walentaite, and to Colin MacRae and Cameron Davidson for the electron microprobe analyses. This research was undertaken in part using the MX2 beamline at the Australian Synchrotron, part of ANSTO, and made use of the Australian Cancer Research Foundation (ACRF) detector. The authors acknowledge help from the beamline scientists for collection of the single-crystal X-ray data.

References

- Bayliss, P., Kolitsch, U., Nickel, E.H., Pring, A. (2010): Alunite supergroup: recommended nomenclature. *Mineral. Mag.*, **74**, 919–927.
- Dunn, P.J., Peacor, D.R., Roberts, W.L., Campbell, T.J., Ramik, R.A. (1984): Walentaite, a new calcium iron arsenate phosphate from the White Elephant Mine, Pringle, South Dakota. *Neues Jahrb. Mineral., Monatsh.*, **1984**, 169–174.
- Farrugia, L.J. (1999): WinGX suite for small-molecule single-crystal crystallography. *J. Applied Crystallogr.*, **32**, 837–838.
- Hawthorne, F.C. (1985): Schneiderhöhnite, $\text{Fe}^{2+}\text{Fe}_2^{3+}\text{As}_5^{3+}\text{O}_{13}$, a densely packed arsenite structure. *Can. Mineral.*, **23**, 675–679.
- Kharisun, T.M.R., Bevan, D.J.M., Pring, A. (1997): The crystal structure of kintoreite, $\text{PbFe}_3(\text{PO}_4)_2(\text{OH}, \text{H}_2\text{O})_6$. *Mineral. Mag.*, **61**, 123–129.
- Mortier, W.J. (1977): Temperature-dependent cation distribution in dehydrated calcium-exchanged mordenite. *J. Phys. Chem.*, **81**, 1334–1338.
- Nickel, E.H. (1987): Tungsten-bearing walentaite from Griffins Find gold deposit, Western Australia. *Aust. Mineral.*, **1987**, 9–12.
- Pluth, J.J., Smith, J.V., Kvick, A. (1985): Neutron diffraction study of the zeolite thomsonite. *Zeolites*, **5**, 74–80.
- Sheldrick, G.M. (2015): Crystal structure refinement with SHELXL. *Acta Crystallogr.*, **C71**, 3–8.
- Wang, X. & Jacobson, A.J. (1999): Crystal structure of the microporous titanosilicate ETS-10 refined from single-crystal X-ray diffraction data. *Chem. Comm.*, 973–974.

Received 26 February 2018

Accepted 11 May 2018

Modified version received 10 May 2018